Technical Notes

TECHNICAL NOTES are short manuscripts describing new developments or important results of a preliminary nature. These Notes cannot exceed 6 manuscript pages and 3 figures; a page of text may be substituted for a figure and vice versa. After informal review by the editors, they may be published within a few months of the date of receipt. Style requirements are the same as for regular contributions (see inside back cover).

Motion of Particles Injected from the Surface into Stagnation-Point Flow

BERNARD OTTERMAN*
Northeastern University, Boston, Mass.

Nomenclature

a = particle radius
c = flowfield constant
k = density ratio ρ/ρ_s
L = transverse force
Re = Reynolds number
S = magnitude of the curl of fluid velocity
t = time
u = horizontal velocity
v = vertical velocity
x = horizontal coordinate
y = vertical coordinate
δ = boundary-layer thickness
ξ = dimensionless x coordinate [Eq. (15)]
η = dimensionless y coordinate [Eq. (14)]
μ = fluid viscosity
ν = kinematic viscosity
θ = dimensionless time [Eq. (15)]

Subscripts

a = based on particle radius
f = fluid
i = injection
p = particle
s = shear or solid
Ω = angular velocity

Introduction

AN understanding of the trajectory small particles in the vicinity of stagnation points is important in such application as blood flow[1] and dust collection.[2] In Ref. 3 the trajectories of spherical nondeformable particles moving towards and colliding with the stagnation surface were determined. Herein, we investigate the motion of solid particles after reflection by or injection from the surface in the vicinity of a two-dimensional stagnation-point flow.

We assume that a viscous but incompressible fluid flows steadily towards the stagnation surface, and that the flowfield is not significantly perturbed by the motion of the solid particles. The latter are assumed to be spherical. We are primarily interested in the motion of the particles within the viscous boundary layer. Because this region is characterized by large velocity gradients we introduce into the analysis particle-fluid forces which result from the action of fluid shear, in addition to interaction forces due to particle-fluid translational velocity and acceleration differences.

Received July 12, 1971; revision received January 31, 1972. The author would like to express his sincere appreciation to Northeastern University for its support which helped to make this investigation possible.

Index category: Fluid Mechanics.

* Assistant Professor of Mechanical Engineering.

Analysis

Saffman[4,5] in a recent study obtained the net force acting on a small translating sphere which is simultaneously rotating in an unbounded, uniform, simple shear flowfield, the translation velocity being parallel to the stream lines. Three independent particle Reynolds numbers arise in the analysis:

$$\text{slip:}\quad (Re)_a = 2a(u_p-u)/\nu \tag{1a}$$

$$\text{shear:}\quad (Re)_s = 4a^2S/\nu \tag{1b}$$

$$\text{rotation:}\quad (Re)_\Omega = 4a^2\Omega/\nu \tag{1c}$$

where, the particle relative velocity (u_p-u) is measured at its center, S is the magnitude of the velocity gradient, and Ω is the magnitude of the angular velocity. The analysis, which is valid when

$$(Re)_a, (Re)_s, (Re)_\Omega \ll 1 \quad \text{and} \quad (Re)_s, (Re)_\Omega \gg (Re)_a{}^2 \tag{2}$$

showed that in addition to Stokes drag force the particle experiences a transverse force given by

$$(L)_s = 6.46a^2(\rho\mu)^{1/2}S^{1/2}(u_p-u) \tag{3}$$

which is due to the combination of slip and shear, and a lift force which is due to rotation given by

$$(L)_\Omega = \pi r a^3\Omega(u_p-u) \tag{4}$$

The latter result was also obtained by Rubinow and Keller.[6] However, Saffman's study shows that unless the rotation speed is very much greater than the rate of shear, and for freely rotating particle $\Omega = 0.5S$, the lift force due to particle rotation is less by an order of magnitude than that due to the slip-shear [Eq. (3)]. Moreover, as $(Re)_a \to 0$ Brenner[7] showed that Saffman's conditions [Eq. (2)] are always met and the Rubinow-Keller theory is inapplicable.

In general for bounded shear flows, Lawler and Lu[8] suggested the following equation:

$$\bar{L} = A\rho a^2[\nu/S]^{1/2}\mathbf{K}\mathbf{x}(\bar{U}_p-\bar{U}) + B\rho a^3\bar{\Omega}x(\bar{U}_p-\bar{U}) \tag{5}$$

where, $\mathbf{K}$ is the curl of the fluid velocity, $\boldsymbol{\Omega}$ is the relative angular vector, and A and B are coefficients whose value depends on the three Reynolds numbers defined by Eq. (1) and the proximity of the particle to the wall. Up to now experimental data for the coefficient A is not available, and its only theoretical predicted value is due to Saffman[5] for the case just described. In light of this incomplete state of the theory we let $A = 6.46$. Consequently, the results we obtain are exact for those particle trajectories for which the assumption of this study apply and for which Eq. (2) is satisfied. For other cases, the results presented are to be interpreted as yielding estimates of the proper order of magnitude.

We obtain the equation of motion for the particle by combining the first term Eq. (5) with Eq. (17.23) of Ref. 9 and by noting that for Hiemenz flow the $S = \partial u/\partial y$, i.e.,

$$\frac{du_p}{dt} = \frac{\alpha(u-u_p)}{\tau_p} + \beta\frac{du}{dt} + \frac{6.46\alpha}{\frac{4}{3}\pi a^3\rho_s}a^2(\rho\mu)^{1/2}\left|\frac{\partial u}{\partial y}\right|^{1/2}(v_p-v) \tag{6}$$

$$\frac{dv_p}{dt} = \frac{\alpha(v-v_p)}{\tau_p} + \beta\frac{dv}{dt} + \frac{6.46}{\frac{4}{3}\pi a^3\rho_s}a^2(\rho\mu)^{1/2}\left|\frac{\partial u}{\partial y}\right|^{1/2}(u-u_p) \tag{7}$$

where, x and y are in the direction parallel and normal to the surface, respectively, and where

$$k = \rho/\rho_s \tag{8}$$

$$\tau_p = 2a^2\rho_s/9\mu \tag{9}$$

$$\alpha = 2/(2+k); \quad \beta = 3k/(2+k) \tag{10}$$

Recall that for frictionless, incompressible, and steady flow the velocity distribution in the neighborhood of the two-dimensional stagnation point, $x = y = 0$, is equal to

$$U = cx; \quad V = -cy \tag{11}$$

Where U is the velocity in x direction (parallel to the wall), V is the velocity in y direction (normal to the wall), and c is a constant. For viscous flow, Hiemenz and Howarth obtained[4]

$$u/U = \phi'(\eta) \tag{12}$$

$$v = -(cv)^{1/2}\phi(\eta) \tag{13}$$

where:

$$\eta = (c/v)^{1/2}y \tag{14}$$

and the functions $\phi(\eta)$, $\phi'(\eta)$ and $\phi''(\eta)$ are given in Table 5.1 of Ref. 10. We now define the following dimensionless variables:

$$\theta = t/\tau_p, \quad \eta = (c/v)^{1/2}y, \quad \xi = (c/v)^{1/2}x, \quad \overset{*}{u} = u/(cv)^{1/2} \tag{15}$$

$$\overset{*}{v} = v/(cv)^{1/2}, \quad \eta_a = (c/v)^{1/2}a, \quad \overset{*}{u}_p = u_p/(cv)^{1/2}, \quad \overset{*}{v}_p = v_p/(cv)^{1/2}$$

where

$$c\tau_p = \tfrac{2}{9}\eta_a{}^2/k \tag{16}$$

The equations of motion for the particle in terms of aforementioned dimensionless variables become:

$$d\overset{*}{u}_p/d\theta = \alpha(\overset{*}{u} - \overset{*}{u}_p) + 0.343\alpha\eta_a|\xi\phi''(\eta)|^{1/2}(\overset{*}{v}_p - \overset{*}{v}) + c\tau_p\beta[\xi\phi'(\eta)^2 - \xi\phi(\eta)\phi''(\eta)] \tag{17}$$

$$d\overset{*}{v}_p/d\theta = (\overset{*}{v} - \overset{*}{v}_p) + 0.343\alpha\eta_a|\xi\phi''(\eta)|^{1/2}(\overset{*}{u} - \overset{*}{u}_p) + c\tau_p\beta\phi(\eta)\phi'(\eta) \tag{18}$$

$$d\xi_p/d\theta = c\tau_p\overset{*}{u}_p \tag{19}$$

$$d\eta_p/d\theta = c\tau_p\overset{*}{v}_p \tag{20}$$

Equations (17–20) were solved numerically by a fourth-order Runge-Kutta method. The details of the technique are presented in Ref. 11. Note that in these equations η_a and k are the only independent parameters, since α, β, and $c\tau_p$ are dependent on the former as indicated by Eqs. (10) and (16).

In the case of frictionless potential flow integration of Eq. (11) gives

$$x = x_0 e^{ct}; \quad y = y_0 e^{-ct} \tag{21}$$

We now define $\tau_f = 1/c$, as the "flowfield time scale," so that

$$x = x_0 e^{t/\tau_f}; \quad y = y_0 e^{-t/\tau_f} \tag{22}$$

Consequently

$$c\tau_p = \frac{\tau_p}{\tau_f} = \frac{\text{velocity equilibration time constant}}{\text{flowfield time scale}} \tag{23}$$

Note that if k is very small α approaches unity and β approaches zero. Moreover, if k is much less than $\eta_a{}^2$, $c\tau_p$ becomes large, and consequently the particle will not be in velocity equilibrium with the flow. If k is large, the apparent mass effect is significant. Finally, if $k \gg \eta_a{}^2$, $c\tau_p$ is small and the particle and the fluid will be in velocity equilibrium. The relationship between $c\tau_p$, $\eta_a{}^2$, and k is given in Table 1.

Results and Discussion

Paradigmatic particle trajectories are presented in dimensionless coordinates ξ, η, and as a function of η_a and $c\tau_p$ in Figs. 1 and 2. Recall that these dimensionless constants are in turn a function of the governing physical parameter of the problem; namely, particle radius and density, fluid density and kinematic viscosity, and flowfield constant c. For purposes of illustration, and in order to make the presented results more meaningful we have computed the relationship between c and η_a for both water and air for the particle sizes given in Tables 2 and 3. The fluid boundary-layer thickness for the cases considered is also indicated. For example, in the case of water at $c = 1$ sec^{-1} the stagnation-point boundary-layer thickness is equal to 7.5×10^{-3} ft. In this case, and for $a = 3.14 \times 10^{-5}$ ft, $\eta_a = 10^{-2}$. Thus, the boundary-layer thickness ($\delta = 2{,}4\eta$) is 120 times the particle diameter. On the other hand, for $c = 10{,}000$ sec^{-1} and particle radius equal to 3.14×10^{-4} ft, the latter is approximately two times as large as the boundary-layer thickness. It should be clear that the analysis presented is not applicable for this case, since the assumption that the particle does not significantly disturb the flowfield would be violated.

Figure 1 illustrates the trajectories of particles injected into the flow from $\eta = \eta_a$ at $\xi = 0.5$ or $\xi = 1.0$ with a dimensionless velocity $\overset{*}{V}_i = 5.0$, where $\overset{*}{V}_i = V_i/(cv)^{1/2}$, as a function of particle size and density ratio. This graph shows that in general in product $c\tau_p$, rather than particle size or density ratio separately, governs the particle trajectory. This is particularly true for cases where significant penetration into the boundary layers occurs, i.e., $c\tau_p > 0.22$. This figure also shows that small variations in dimensionless particle injection location do not significantly alter the general nature of the particle trajectory. In this connection recall that $\xi = (c/v)^{1/2}x$. Consequently, a specified value of ξ, corresponds to different dimensional injection location as the velocity flowfield and/or type of fluid are varied.

Figure 2 gives the maximum distance penetrated by particles into the boundary layer, η_m, as a function of injection velocity for particles of different size and density. Particle injection took place at $\xi = 0.50$, $\eta = \eta_a$. As this figure indicates, when $\overset{*}{V}_i > 1$, η_m is a linear function of $\overset{*}{V}_i$ for a given $c\tau_p$ and η_a. Moreover,

Table 2 Relations among c, δ, η_a, and a for water at temperature of 80°F

c, sec^{-1}	δ, ft	η_a			
		$a = 3.14 \times 10^{-7}$ ft	$a = 3.14 \times 10^{-6}$ ft	$a = 3.14 \times 10^{-5}$ ft	$a = 3.14 \times 10^{-4}$ ft
10000	7.5×10^{-5}	10^{-2}	10^{-1}	1	10
100	7.5×10^{-4}	10^{-3}	10^{-2}	10^{-1}	1
1	7.5×10^{-3}	10^{-4}	10^{-3}	10^{-2}	10^{-1}
0.01	7.5×10^{-2}	10^{-5}	10^{-4}	10^{-3}	10^{-2}

Table 3 Relations among c, δ, η_a, and a for air at temperature of 80°F

c, sec^{-1}	δ, ft	η_a			
		$a = 3.14 \times 10^{-6}$ ft	$a = 3.14 \times 10^{-5}$ ft	$a = 3.14 \times 10^{-4}$ ft	$a = 3.14 \times 10^{-3}$ ft
10000	3.1×10^{-4}	10^{-2}	10^{-1}	1	10
100	3.1×10^{-3}	10^{-3}	10^{-2}	10^{-1}	1
1	3.1×10^{-2}	10^{-4}	10^{-3}	10^{-2}	10^{-1}
0.01	3.1×10^{-1}	10^{-5}	10^{-4}	10^{-3}	10^{-2}

Table 1 Relations among $c\tau_p$, η_a, and k

k / η_a	100	10	1	0.1	0.01	0.001	0.0001	0.00001
	$k/c\tau_p$							
1	$2/9 \times 10^{-2}$	$2/9 \times 10^{-1}$	$2/9 \times 10^{+0}$	$2/9 \times 10$	$2/9 \times 10^{2}$	$2/9 \times 10^{3}$	$2/9 \times 10^{4}$	$2/9 \times 10^{5}$
0.1	$2/9 \times 10^{-4}$	$2/9 \times 10^{-3}$	$2/9 \times 10^{-2}$	$2/9 \times 10^{-1}$	$2/9 \times 10^{+0}$	$2/9 \times 10$	$2/9 \times 10^{2}$	$2/9 \times 10^{3}$
0.01	$2/9 \times 10^{-6}$	$2/9 \times 10^{-5}$	$2/9 \times 10^{-4}$	$2/9 \times 10^{-3}$	$2/9 \times 10^{-2}$	$2/9 \times 10^{-1}$	$2/9 \times 10^{+0}$	$2/9 \times 10$
0.001	$2/9 \times 10^{-8}$	$2/9 \times 10^{-7}$	$2/9 \times 10^{-6}$	$2/9 \times 10^{-5}$	$2/9 \times 10^{-4}$	$2/9 \times 10^{-3}$	$2/9 \times 10^{-2}$	$2/9 \times 10^{-1}$
0.0001	$2/9 \times 10^{-10}$	$2/9 \times 10^{-9}$	$2/9 \times 10^{-8}$	$2/9 \times 10^{-7}$	$2/9 \times 10^{-6}$	$2/9 \times 10^{-5}$	$2/9 \times 10^{-4}$	$2/9 \times 10^{-3}$

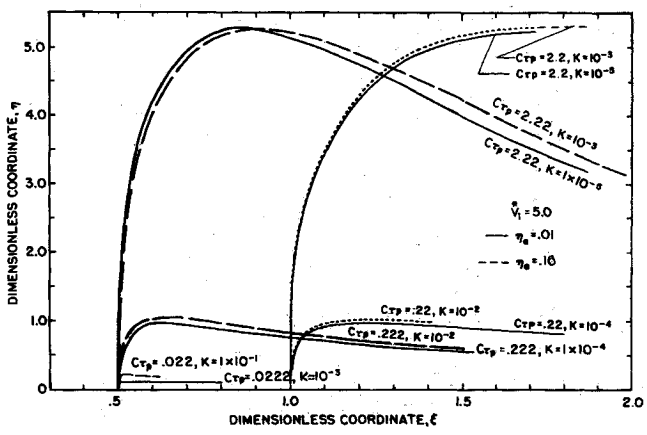

Fig. 1 Particle trajectories for the case of $V_i^* = 5.0$.

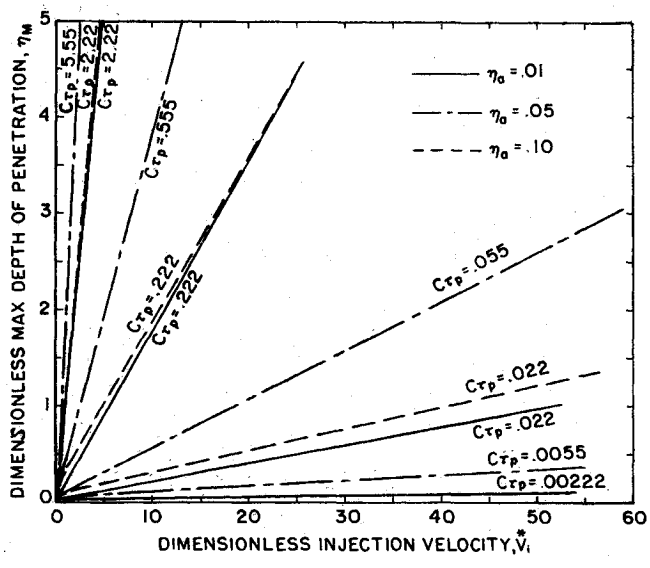

Fig. 2 Maximum penetration depth as a function of injection velocity.

for $c\tau_p > 0.10$, η_m is, for all practical purposes, independent of η_a and for a given $c\tau_p$ is determined only by V_i^*. Recall that for Hiemenz flow, the edge of the boundary layer corresponds to $\eta \simeq 2.4$. Consequently, Fig. 2 automatically yields, for a given $c\tau_p$, the dimensionless injection velocity required to reach the edge of the boundary layer.

References

[1] Petscheck, H., Adamis, D., and Kantrowitz, A. R., "Stagnation Flow Thrombus Formation," *Transactions of the American Society of Artificial Internal Organs*, Vol. 14, 1968, pp. 256–259.

[2] Fuchs, N. A., *Mechanics of Aerosols*, Pergamon Press, London, 1964.

[3] Otterman, B and Yau, F., "Motion of Small Particles within the Stagnation of Region of a Viscous-Incompressible Fluid," *Proceedings of the Society of Engineering Science*, 8th Annual Meeting, Washington, D.C., 1970.

[4] Saffman, P. G., "The Lift on a Small Sphere in a Slow Shear Flow," *Journal of Fluid Mechanics*, Vol. 22, Pt. 2, 1965, pp. 385–400.

[5] Saffman, P. G., "Corrigendum," *Journal of Fluid Mechanics*, Vol. 31, Pt. 3, 1968, p. 624.

[6] Rubinow, S. I. and Keller, J. B., "The Transverse Force on a Spinning Sphere Moving in a Viscous Fluid," *Journal of Fluid Mechanics*, Vol. 11, 1961, pp. 447–459.

[7] Brenner, H., *Advances in Chemical Engineering*, Vol. 6, Academic Press, New York, 1966.

[8] Lawler, M. T. and Lu, P. C., "A Study of Radial Migrations in Fluid-Particle Flows with Fluid Rotation," *Advances in Solid-Liquid Flows in Pipes and Its Application*, edited by I. Zandi, Pergamon Press, New York, 1971.

[9] Fuchs, N. A., *Mechanics of Aerosols*, Pergamon Press, London, 1964, p. 75.

[10] Schlichting, H., *Boundary Layer Theory*, McGraw-Hill, New York, 1955.

[11] Yau, F. F. P., "Motion of Particles in Laminar Flows of Solid-Fluid Mixtures," M.S. thesis, 1970, Dept. of Mech. Engineering, Northeastern Univ., Boston, Mass.

Hypersonic Viscous, Slip Flow over Insulated Wedges

AJAY KUMAR* AND A. C. JAIN†

Indian Institute of Technology, Kanpur, India

Nomenclature

c	$= \mu_w T_\infty / \mu_\infty T_w$, Chapman-Rubesin constant
c_f	$= \tau / \frac{1}{2}\rho_\infty u_\infty^2$
C_p	= specific heat at constant pressure
H	= total enthalpy
k	= thermal conductivity
M	= Mach number
p, ρ, T	= pressure, density, and temperature, respectively
Pr	= Prandtl number
R	= gas constant
Re_x	$= u_\infty \rho_\infty x / \mu_\infty$
u, v	= velocity components along x, y directions
u_b	= slip velocity
x, y	= distances along and perpendicular to the wedge surface
ξ, η	= defined in Eq. (12)
β	= semiwedge angle
γ	= ratio of specific heats
δ	= boundary-layer thickness
θ_s	$= \beta + d\delta/dx$, local slope of the boundary-layer edge with free-stream
λ	= mean free path
τ	$= \mu_w (\partial u/\partial y)_w$
μ	= coefficient of viscosity
$\bar{\chi}$	$= M_\infty^3 (c/Re_x)^{1/2}$, strong interaction parameter

Subscripts

∞	= conditions in freestream
e	= conditions at the edge of the boundary layer
w	= conditions at the wall

Introduction

SHEN[1] investigated the hypersonic flow past an insulated wedge with no slip boundary conditions at the surface. He found that boundary-layer thickness varies as $(x)^{3/4}$ and pressure ratio (p_w/p_∞) varies as $(x)^{-1/2}$. This indicates that pressure ratio tends to infinity as leading edge is approached. Aroesty[2] investigated the slip effects in the strong interaction region by taking slip velocity as a perturbation to the no slip case. Here, we modified Shen's solution over the wedge by incorporating the effect of slip velocity at the surface. An inviscid flow is envisaged in between the shock wave and the boundary layer. Tangent-wedge approximation provides the pressure distribution at the

Received August 4, 1971; revision received March 2, 1972. This work was supported by the Ministry of Defence, Government of India, under a Grant-in-Aid Project entitled "Hypersonic Flow at Low Reynolds Numer."

Index category: Supersonic and Hypersonic Flow.

* Senior Research Fellow, Department of Aeronautical Engineering.

† Assistant Professor, Department of Aeronautical Engineering.